Improving Language Transfer Capability of Decoder-only Architecture in Multilingual Neural Machine Translation

Zhi Qu[†] **Yiran Wang**[‡] **Chenchen Ding**[†‡]
Hideki Tanaka[‡] **Masao Utiyama**[‡] **Taro Watanabe**[†]
[†]Nara Institute of Science and Technology, Japan
{qu.zhi.pv5, taro}@is.naist.jp
[‡]National Institute of Information and Communications Technology, Japan
{yiran.wang, chenchen.ding, hideki.tanaka, mutiyama}@nict.go.jp

Abstract

Existing multilingual neural machine translation (MNMT) approaches mainly focus on improving models with the encoder-decoder architecture to translate multiple languages. However, decoder-only architecture has been explored less in MNMT due to its underperformance when trained on parallel data solely. In this work, we attribute the issue of the decoder-only architecture to its lack of language transfer capability. Specifically, the decoder-only architecture is insufficient in encoding source tokens with the target language features. We propose dividing the decoding process into two stages so that target tokens are explicitly excluded in the first stage to implicitly boost the transfer capability across languages. Additionally, we impose contrastive learning on translation instructions, resulting in improved performance in zero-shot translation. We conduct experiments on TED-19 and OPUS-100 datasets, considering both training from scratch and fine-tuning scenarios. Experimental results show that, compared to the encoder-decoder architecture, our methods not only perform competitively in supervised translations but also achieve improvements of up to 3.39 BLEU, 6.99 chrF++, 3.22 BERTScore, and 4.81 COMET in zero-shot translations. We release our codes at https://github.com/zhiqu22/PhasedDecoder.

1 Introduction

Multilingual neural machine translation (MNMT) (Firat et al., 2016) aims to integrate multiple language translation directions into a single model. Although multilingual translation systems based on large language models have demonstrated strong performance (Zhang et al., 2023; Yang et al., 2023; Xu et al., 2024), current MNMT models with the encoder-decoder architecture (Fan et al., 2020; Goyal et al., 2022; Team et al., 2022) remain a focus of research due to the competitive performance, fewer parameters, and reduced training costs (Zhu et al., 2023). However, in MNMT, models with the decoder-only architecture[1] have shown underperformance by the empirical research of Gao et al. (2022); Zhang et al. (2022), as further evidenced by Figure 1a. Therefore, addressing the underdevelopment of decoder-only architectures in MNMT is crucial due to the advantage of zero-shot generalization (Wang et al., 2022), which potentially benefits zero-shot translation, i.e., translating language pairs unseen during training.

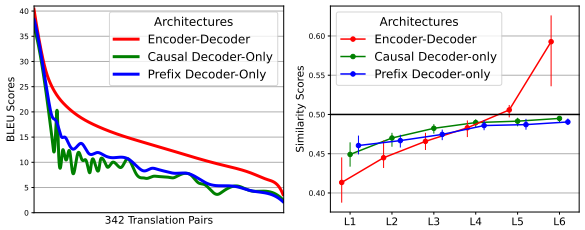

(a) Performance (b) Language Feature

Figure 1: Comparison between different architectures in preliminary experiments on TED-19. Figure 1a shows the BLEU score. Figure 1b shows the layer-wise language feature representations of a sentence where the x-axis indicates the layer number and the vertical line indicates the value range. Specifically, we follow Qu et al. (2024) to compute a similarity score, where values higher than 0.5 mean the representation exhibits the target language features more and lower than 0.5 indicates showing more source language features. Appendix A provides the details of implementation.

We attribute the issue to the lack of language transferability, causing generations to rely solely on representations that always manifest the source language features. Specifically, MNMT encoder-decoder models typically add a language tag indicating the target language at the beginning of the source tokens as a translation instruction (Johnson et al., 2017; Wu et al., 2021), then, Kudugunta et al. (2019); Qu et al. (2024) show that the encoder of MNMT models transfers source tokens to represent

[1]The term "decoder-only architecture" encompasses both causal decoder-only architectures (Radford et al., 2018) and prefix decoder-only architectures (Dong et al., 2019).

Proceedings of the 5th Workshop on Multilingual Representation Learning (MRL 2025), pages 178–195
November 8-9, 2025

target language features more than source language features. As shown in Figure 1b, the representation of source tokens extracted from the model with the encoder-decoder architecture mainly exhibits the target language features at the output of the encoder (red line), however, this characteristic is absent in decoder-only architectures (green and blue lines). We hypothesize that the decoder-only architectures merely capture the surface information of source tokens instead of transferring source tokens into a state with more target language features.

We propose dividing the decoder-only architecture into two stages, namely, Two-stage Decoder-only (TDO). Specifically, the representations of target tokens are excluded in the first stage to enforce language transfer using the translation instruction, and the target tokens are fused in the second stage, which follows the normal decoder-only manner. Moreover, unlike the encoder-decoder architecture, where source and target tokens are processed separately, in the decoder-only architecture, source tokens pass through all layers. However, the training objective of MNMT only focuses on the target tokens, leading to the degradation of the target language features on the source token representation. Thus, we introduce Instruction-level Contrastive Learning (InstruCL) as a training objective to supervise source tokens in the second stage.

We evaluate the proposed methodologies on two datasets, TED-19 (Ye et al., 2018), and OPUS-100 (Zhang et al., 2020a; Yang et al., 2021), using four automatic evaluation metrics: BLEU (Papineni et al., 2002; Post, 2018), chrF++ (Popović, 2015, 2017), BERTScore (Zhang et al., 2020b) and COMET (Rei et al., 2020). Experimental results show that, compared to encoder-decoder models, our models perform competitively in supervised translations and achieve improvements of up to 3.39 BLEU, 6.99 chrF++, 3.22 BERTScore, and 4.81 COMET in zero-shot translations. We also analyze the variation of layer-wise representations at the sentence level to demonstrate the effects of our proposed methods. Results prove that the gains of proposed methods in the decoder-only architecture derived from improving language transfer.

2 Related Work

Although the large language model based on the decoder-only architecture performs satisfactorily in the multilingual translation (Zhu et al., 2023; Xu et al., 2024), the SOTA models specialized on MNMT are still based on the encoder-decoder architecture (Fan et al., 2020; Team et al., 2022) due to the balance between costs and performances. Gao et al. (2022); Zhang et al. (2022) empirically show that the decoder-only architecture does not have a distinct advantage in MNMT, and Dabre et al. (2020); Raffel et al. (2023) demonstrate that the reason could be the onefold style of training data comprising only translations, degrading the zero-shot ability of the decoder-only architecture (Brown et al., 2020; Wang et al., 2022).

Recent investigations of the encoder-decoder architecture in MNMT reveal the deficiency of the decoder-only architecture at the representation level. Kudugunta et al. (2019); Stap et al. (2023) point out that the sentence representations translating to two different target languages are gradually separated with the increase of layers. Qu et al. (2024) demonstrate that the encoder of MNMT model transfers the source sentence representation to the target side, leading to the representation of source tokens used in the generation with more target language features. This finding aligns with the prior empirical studies (Wu et al., 2021; Qu and Watanabe, 2022; Pires et al., 2023), which shows that increasing target language information can lead to performance improvements. Moreover, this also supports our hypothesis that the weakness of the decoder-only architecture can be attributed to the lack of language transfer.

3 Backgrounds

3.1 Multilingual Neural Machine Translation

A parallel multilingual corpus, denoted by $\mathbb{C}$, consists of translation pairs in the form of $(\boldsymbol{x}, \boldsymbol{y})$. Here, $\boldsymbol{x} = x_1, \ldots, x_I$ is the source sentence comprising I tokens, and $\boldsymbol{y} = y_1, \ldots, y_J$ is the target sentence with J tokens. We also denote language tags by $\boldsymbol{l} = l_1, \ldots, l_K$, where each tag is an artificial token uniquely corresponding to one of the K languages in $\mathbb{C}$. To serve as a translation instruction, we add the language tag specifying the target language at the beginning of the source tokens (Johnson et al., 2017; Wu et al., 2021), denoted by $l_{\boldsymbol{y}}$.[2] Thus, the training data comprises instances in the form of $(l_{\boldsymbol{y}}, \boldsymbol{x}, \boldsymbol{y})$. The model is trained over all instances in $\mathbb{C}$ by the standard cross-entropy objective:

$$\mathcal{L}_{\text{ce}} = -\sum_{l_{\boldsymbol{y}}, \boldsymbol{x}, \boldsymbol{y} \in \mathbb{C}} \sum_{j=1} \log\ p(y_j \mid l_{\boldsymbol{y}}, \boldsymbol{x}, \boldsymbol{y}_{<j}), \quad (1)$$

[2]Appendix B shows the comparison between different strategies of translation instructions in MNMT.

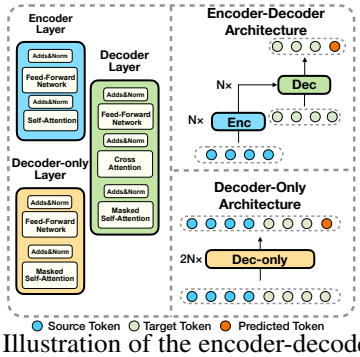

Figure 2: Illustration of the encoder-decoder architecture and the decoder-only architecture.

where $p(y_j \mid l_{\boldsymbol{y}}, \boldsymbol{x}, \boldsymbol{y}_{<j})$ is a probability distribution for each token generated by MNMT model.

3.2 Architectures

All architectures discussed in this work follow the Transformer architecture (Vaswani et al., 2017), and almost all MNMT models are based on the encoder-decoder architecture (Johnson et al., 2017; Fan et al., 2020; Team et al., 2022; Raffel et al., 2023), as illustrated in Figure 2. It comprises an encoder and a decoder in which both are composed of N layers with each encoder layer comprising a self-attention mechanism and a feed-forward network (FFN), and with each decoder layer comprising a masked self-attention mechanism, a cross-attention mechanism, and an FFN. The encoder receives $I+1$ tokens combining by $(l_{\boldsymbol{y}}, \boldsymbol{x})$[3], and output the representations $\mathbf{H} = \{\boldsymbol{h}_1, ..., \boldsymbol{h}_{I+1}\}, \boldsymbol{h} \in \mathbb{R}^d$, d is the model dimension. Then, the decoder relies on $\mathbf{H}$ and $\boldsymbol{y}_{<j}$ to generate the next token:

$$\mathbf{H}^N = \text{encoder}(l_{\boldsymbol{y}}, \boldsymbol{x}), \tag{2}$$

$$y_j = \text{decoder}(\mathbf{H}^N, \boldsymbol{y}_{<j}), \tag{3}$$

where $\mathbf{H}^N$ is an intermediate state used in the cross-attention mechanism in each decoder layer without further transformation. Thus, Equation 1 implicitly aligns the output of the encoder in the representational subspace of the target language, i.e., the language transfer as shown in the red line of Figure 1b, because the ideal decoder should translate two sentences $\boldsymbol{x}^a$ and $\boldsymbol{x}^b$, which have the same target language, parallel semantics, and different source languages, to the same target sentence $\boldsymbol{y}$. Formally, an ideal encoder meets the following:

$$\text{encoder}(l_{\boldsymbol{y}}, \boldsymbol{x}^a) = \text{encoder}(l_{\boldsymbol{y}}, \boldsymbol{x}^b). \tag{4}$$

A decoder-only architecture refers to a model that consists solely of a decoder (Figure 2). Each decoder-only layer consists of a masked self-attention mechanism and an FFN (Radford et al., 2018), and each model has $2N$ layers to approximately match the parameter size of an encoder-decoder architecture. We define the decoder-only process as follows:

$$y_j = \text{decoder-only}(l_{\boldsymbol{y}}, \boldsymbol{x}, \boldsymbol{y}_{<j}). \tag{5}$$

Notably, the difference between $\text{decoder-only}(\cdot)$ and $\text{decoder}(\cdot)$ is that $\text{decoder-only}(\cdot)$ fuses the source and target information by a concatenated input, namely, $l_{\boldsymbol{y}}$, $\boldsymbol{x}$, and $\boldsymbol{y}$ are equally treated[4], instead of using a cross-attention mechanism. Thus, there exists no intermediate state to align different source languages as Equation 4, resulting in the blue and green lines of Figure 1b. Moreover, we follow Gao et al. (2022); Raffel et al. (2023) to distinguish the decoder-only by the manner of masked self-attention mechanism as causal decoder-only and prefix decoder-only (Appendix D). Finally, compared to the encoder-decoder architecture, the decoder-only architecture requires around 10% fewer parameters (Appendix E).

4 Methodologies

4.1 Two-stage Decoder-only Architecture

The limitations of the decoder-only architecture in MNMT likely arise from inadequate language transfer capabilities, i.e., the absence of Equation 4. To address this issue, we propose the Two-stage Decoder-only (TDO) architecture, which divides the decoder-only process into two stages to implicitly align representations of different source languages in the subspace of the target language. Specifically, as illustrated in Figure 3, the target tokens are explicitly excluded in the first stage, i.e., the first M layers, and these target tokens are fused in the second stage, i.e., the subsequent $2N - M$ layers. The process of TDO is formally expressed:

$$\mathbf{H}^M = \text{decoder-only}_1(l_{\boldsymbol{y}}, \boldsymbol{x}), \tag{6}$$

$$y_j = \text{decoder-only}_2(\mathbf{H}^M, \boldsymbol{y}_{<j}), \tag{7}$$

where $\text{decoder-only}_1(\cdot)$ enables the implicit alignment as done in Equation 4. Notably, the first stage logically acts as an encoder when prefixed masking is applied to the self-attention mechanism. However, the first and second stages remain unified structures, and the fusing of source and target information follows the manner of $\text{decoder-only}(\cdot)$

[3]The operation of combining means adding $l_{\boldsymbol{y}}$ at the beginning of $\boldsymbol{x}$. Appendix C shows the specific forms in detail.

[4]Appendix C compares the difference of the input and output forms between encoder-decoder and decoder-only models.

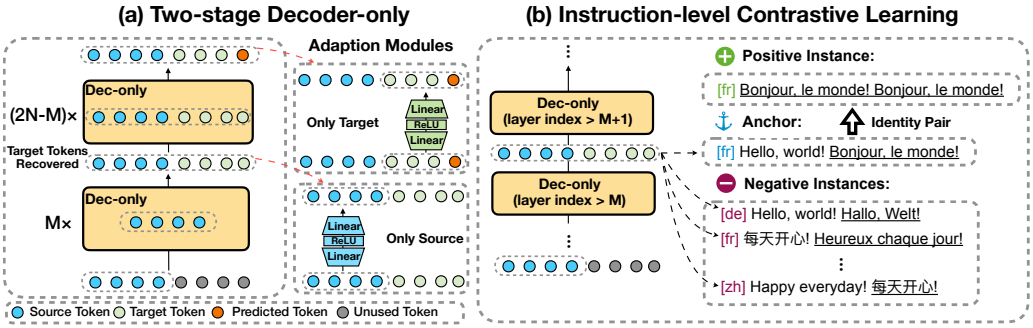

Figure 3: Illustration of proposed methods. Notably, the term, Token, not only means the real token before and after the processing of model, but also refers to the representation in the corresponding position. (a) shows the Two-stage Decoder-only and shows the Adaption, i.e., using an additional FFN to narrow the gap between source and target representations by non-linear transformation. (b) shows the Instruction-level Contrastive Learning. Underline marks target tokens, and [*] means the instruction of this instance. For the anchor, negative instances in this figure meet at least one of two features: 1) different target language and 2) unparallel semantics.

rather than $\mathrm{decoder}(\cdot)$. Therefore, TDO architecture preserves the decoder-only architecture.

Notably, a representational gap arises at the $M+1$ layer due to our imbalance design where the source tokens have passed through the preceding M layers, while the target tokens are not. To bridge this gap, as shown in Figure 3, we employ an additional FFN as an adaption module[5] at the output of the M layer to nonlinearly transform the representation of source tokens. Similarly, since the source and target tokens share the same representational space in the second stage, we employ another adapter at the output of the $2N$ layer to ensure that the output representation of target tokens remains unaffected by the source language.

4.2 Instruction-level Contrastive Learning

Although Equation 6 transfers $\mathbf{H}$, i.e., the representation of source tokens, to $\mathbf{H}^M$, which aligns with the target language, $\mathbf{H}$ potentially tends to degrade towards the source language in Equation 7 because Equation 1 does not supervise $\mathbf{H}$ directly.[6]

Contrastive learning, which is a technique to encourage representations towards the target states (Jaiswal et al., 2021), is helpful to mitigate this degradation. However, two challenges remain in this process. The first is the lack of optimization objectives for aligning $\mathbf{H}$ with the target language. For instance, the $\mathbf{H}$ derived by a translation from German to English cannot be considered an anchor to optimize another $\mathbf{H}$ derived by a translation from French to English because neither adequately represents the optimal state of English. The second challenge is that the optimization at the sentence representation level potentially leads to suboptimal results. For instance, Pan et al. (2021) suggest averaging representations of all tokens to get a sentence representation for contrastive learning, which loses the syntactic information.

We propose Instruction-level Contrastive Learning (InstruCL), which only aligns $l_{\boldsymbol{y}}$, i.e., the translation instruction, of each instance, given that MNMT remains sensitive to $l_{\boldsymbol{y}}$ (Wu et al., 2021). As shown in Figure 3, given an anchor $(l_{\boldsymbol{y}}, \boldsymbol{x}, \boldsymbol{y})$, we establish an identity pair in the form of $(l_{\boldsymbol{y}}, \boldsymbol{y}, \boldsymbol{y})$, namely a pseudo pair translating the target sentence to itself, as the positive instance because the identity pair can serve as a proxy for the target language (Qu et al., 2024). Specifically, in a training batch, we have a set of representations $\mathbb{B} = \{\boldsymbol{h}_1^1, \boldsymbol{h}_1^2, \dots\}$ where $\boldsymbol{h}_1$ is the representation of $l_{\boldsymbol{y}}$ collected from $\mathbf{H}$. Then, we designate one instance of $\mathbb{B}$ as the anchor, denoted by $\boldsymbol{h}^{\text{anc}}$. Other instances are treated as negative instances, which meet one or both of the following features compared to the anchor: different target languages or unparallel semantics. Subsequently, the identity pair established by the anchor would be fed into the model and we collect the representation of $l_{\boldsymbol{y}}$ at the same layer, and denote it by $\boldsymbol{h}^{\text{pos}}$. The objective of InstruCL is formulated as:

$$\begin{aligned}
\mathcal{L}_{\text{ctr}} &= -\sum_{\boldsymbol{h}\in\mathbb{B}} \log \frac{\exp(s^+)}{\exp(s^+) + \sum_{i=1}^{|\mathbb{B}|-1} \exp(s_i^-)}, \\
s^+ &= \mathrm{sim}(\boldsymbol{h}^{\text{anc}}, \boldsymbol{h}^{\text{pos}}), \\
s_i^- &= \mathrm{sim}(\boldsymbol{h}^{\text{anc}}, \boldsymbol{h}_1^i), \boldsymbol{h}_1^i \neq \boldsymbol{h}^{\text{anc}},
\end{aligned} \tag{8}$$

where $\mathrm{sim}(\cdot)$ calculates the similarity of representa-

[5] Adaptation module is shared for all languages instead of a language-specific component (Bapna and Firat, 2019).

[6] Although the language modeling loss (Radford et al., 2018) can provide supervision for the representation of source tokens, Gao et al. (2022) show that supervising the representation of source tokens does not benefit MNMT.

tions using the cosine similarity. The final training objective is simply jointed as:

$$\mathcal{L} = \mathcal{L}_{\text{ce}} + \mathcal{L}_{\text{ctr}}. \quad (9)$$

5 Experiments

5.1 Datasets and Evaluations

Following prior works (Wu et al., 2021; Zhang et al., 2022; Tan and Monz, 2023; Stap et al., 2023; Qu et al., 2024), we use English-centric datasets in our experiments, where the training and validation data consist of translation pairs both from English and to English. It is an ideal setup for the evaluation of zero-shot translation capabilities, because non-central languages have never seen each other. We utilize two datasets in our experiments: 1) TED-19 (Qu et al., 2024), a sub-collection of TED Talks (Ye et al., 2018), comprising 6.5 million instances across 19 languages from various language families; and 2) OPUS-100 (Zhang et al., 2020a; Yang et al., 2021), which includes 95 languages and a total of 92 million instances. Detailed information about these datasets is provided in Appendix F.

We set the beam size to 4 during inference and evaluate the output quality using four automatic evaluation metrics for a comprehensive assessment: SacreBLEU (Papineni et al., 2002; Post, 2018), chrF++ (Popović, 2015, 2017), BERTScore (Zhang et al., 2020b), and COMET (Rei et al., 2020). Moreover, we measure the target-off ratio on zero-shot pairs, i.e., the ratio of cases where the source sentence is not translated into the correct target language, as a secondary metric. Finally, we conduct statistical significance testing for zero-shot pairs by using paired bootstrap resampling (Koehn, 2004). The settings of these evaluation metrics are described in Appendix G.

5.2 Experimental Setups

We conduct experiments from two perspectives: training from scratch and fine-tuning. Based on the findings by Gao et al. (2022); Zhang et al. (2022), which empirically demonstrate that the decoder-only architecture underperforms compared to the encoder-decoder architecture in MNMT, and our motivation, which aims to improve the decoder-only architecture, our baselines are vanilla models with the encoder-decoder and decoder-only architectures. Specifically, we train models with the encoder-decoder architecture from scratch using TED-19 and OPUS-100 as baselines. Additionally, we fine-tune three pre-trained models with the encoder-decoder architecture: M2M-418M (Fan et al., 2020), NLLB-600M (Team et al., 2022), and M2M-1.2B (Fan et al., 2020), in TED-19. Moreover, although the proposed methods are not restricted to a specific architecture, the adaptation modules are not implemented for the models with the encoder-decoder architecture, because, when the hyper-parameters are consistent, the decoder-only architecture with adaptation modules still contains fewer learnable parameters[7] to ensure fairness, i.e., models have the same magnitude of parameters. In addition to discussing the parameters, we further discuss the impact of computational complexity in Appendix J. Finally, we conduct experiments that apply InstruCL to models with different architectures, and we provide the experimental results and discussions in Appendix I as assisted evidence to support the motivation in Section 4.2, namely, InstruCL supplements the inadequate supervision of Equation 1 in the second stage.

Our models in this work conform to the manner of the Transformer (Vaswani et al., 2017). For training from scratch, we configure the models with $N = 6$, $d = 512$, and an FFN inner size of $4d$ for models trained on TED-19. The FFN in the adaptation module is dimensionally matched to the FFN in the main network. For OPUS-100, we explore both a deeper model with $N = 12$ and a wider model with $N = 6$ and $d = 1024$. Fine-tuning experiments are conducted solely on TED-19. Given that pre-trained models for MNMT typically employ an encoder-decoder architecture, we initialize our model's parameters from the decoder, freezing the embedding layer during training. For M2M-418M and NLLB-600M, we set $N = 6$, and for M2M-1.2B, we set $N = 12$, maintaining the original settings for d and the FFN inner size. To ensure comparability across different architectures, we consistently set $M = N$ and the layer index of InstruCL to $1.5N$ in the main experiments. Detailed settings for training and the count of learnable parameters can be found in Appendix H.

5.3 Results: Training from scratch

Table 1 shows the experimental results. The comparison between the basic architectures shows that, first, the prefix decoder-only consistently outperforms the causal decoder-only, which aligns with Raffel et al. (2023). Second, the decoder-only architecture consistently underperforms the encoder-

[7] Appendix H lists the count of modeling parameters for different cases in detail.

					BLEU ↑			chrF++ ↑			BERTScore ↑			COMET ↑			off ↓
		Pref.	Adap.	CL	en→	→en	zero	en→	→en	zero	en→	→en	zero	en→	→en	zero	zero
TED N=6 d=512	Enc-Dec				25.46	28.31	12.32	45.96	50.86	32.13	84.10	93.37	78.03	80.49	78.15	67.26	3.82
	Dec-only				22.54	24.14	7.33	42.84	45.08	23.36	82.96	92.31	74.38	76.60	72.99	57.50	6.01
		✓			24.00	26.97	8.18	44.49	48.93	25.35	83.54	92.97	74.52	78.46	76.10	56.74	5.51
	TDO				25.47	28.88	13.56	45.98	51.33	34.04	84.11	93.45	78.90	80.41	78.42	69.74	3.54
			✓		25.55	**28.98**	13.61	46.03	**51.49**	34.11	84.15	93.50	78.94	80.56	**78.65**	70.09	3.49
				✓	25.37	28.46	13.95†	45.99	51.13	34.41†	84.09	93.40	79.15	80.35	78.26	70.43†	3.45
			✓	✓	25.60	28.82	14.16†	46.11	51.35	34.76†	84.13	93.45	79.29†	80.52	78.47	70.98†	3.43
		✓			25.53	28.76	14.26†	46.01	51.09	34.72†	84.13	93.41	79.27†	80.43	78.18	70.82†	3.43
		✓	✓		25.61	28.52	14.51†	46.04	50.89	35.01†	**84.16**	93.40	79.41†	80.60	78.16	71.48†	3.49
		✓		✓	**25.62**	28.94	14.70†	**46.15**	51.46	35.34†	84.15	**93.47**	79.57†	80.55	78.55	71.94†	**3.39**
		✓	✓	✓	25.61	28.66	**14.81**†	46.05	51.01	**35.35**†	**84.16**	93.41	**79.60**†	**80.61**	78.22	**72.07**†	3.42
OPUS N=12 d=512	Enc-Dec				**25.18**	29.79	5.13	**44.75**	48.40	12.95	**82.98**	92.33	72.44	**76.59**	76.21	58.51	64.21
	Dec-only				23.09	26.80	5.42	42.18	45.05	13.55	82.19	91.72	72.48	74.66	73.65	58.17	60.22
		✓			23.96	28.41	6.62	42.98	47.22	15.36	82.47	92.06	73.57	75.48	75.34	**59.56**	58.91
	TDO	✓			24.88	**29.97**	5.32	44.72	**49.39**	13.29	82.91	**92.41**	72.50	76.26	**76.73**	58.30	51.56
		✓	✓		24.79	29.22	5.97	44.69	48.35	14.30	82.87	92.34	72.97	76.04	76.25	58.33	53.80
		✓		✓	24.35	29.52	7.93†	44.44	48.74	18.65†	82.84	92.37	73.97	75.93	76.23	58.71	48.37
		✓	✓	✓	24.73	29.70	**8.52**†	44.60	48.72	**19.94**†	82.90	92.38	**74.32**†	76.16	76.59	58.82	**43.38**
OPUS N=6 d=1024	Enc-Dec				**27.71**	31.60	6.95	46.84	50.31	15.89	83.55	92.62	74.12	**78.10**	77.58	59.99	57.15
	Dec-only				26.09	29.09	7.55	44.51	47.44	16.98	82.93	92.12	73.94	76.77	75.80	61.21	63.80
		✓			26.79	30.42	8.15	45.48	48.92	17.65	83.21	92.37	74.17	77.53	76.69	**62.32**	55.67
	TDO	✓			27.22	31.58	7.06	46.54	**50.59**	15.96	83.44	92.64	73.78	77.68	**77.89**	60.60	52.43
		✓	✓		27.51	**31.64**	7.70	**46.87**	50.39	17.32	**83.58**	92.58	74.32	78.05	77.58	61.24	49.87
		✓		✓	27.12	31.49	9.28†	46.55	50.23	**21.33**†	83.50	**92.65**	**75.04**†	77.63	77.64	60.84	**39.71**
		✓	✓	✓	27.45	31.36	**9.36**†	46.79	50.06	21.05†	83.52	92.64	74.88†	77.97	77.75	61.78†	43.36

Table 1: Averaged scores of results in the experiments of training from scratch. Enc-Dec and Dec-only are abbreviations of encoder-decoder and decoder-only, respectively. Pref., Adap., and Cl abbreviates Prefix, Adaption and InstruCL, respectively. ✓in the Prefix column means the masked self-attention mechanism follows Prefix manner, conversely, follows Causal manner. en→ and →en means the supervised pairs translating from English to non-central languages and translating from non-central languages to English, respectively. zero abbreviates zero-shot pairs, off abbreviates the target-off ratio. The best score in each column and block is in bold and the numbers with † are significantly better than Enc-Dec according to the significance test with $p < 0.1$.

decoder architecture in supervised pairs of all three settings, with maximum deficits of -4.17, -5.78, -1.14, and -5.16 on the BLEU, chrF++, BERTScore, and COMET respectively. On the other hand, while the decoder-only architecture shows weaker performance on TED-19 for zero-shot translation, it achieves higher scores in two settings on OPUS-100. This suggests that the zero-shot capability of the decoder-only architecture in MNMT relates to the amount of data and parameters.

In comparison with the encoder-decoder architecture, TDO first achieves competitively supervised capabilities using fewer parameters. Second, our method exhibits stronger zero-shot translation scores, achieving scores improvements of +2.49, +3.22, +1.57, and +4.81; +3.39, +6.99, +1.88, and +0.31; +2.41, +5.16, +0.76, +1.79 across three settings respectively. Meanwhile, the results of significance testing endorse that our proposed methods can resolve inadequate language transfer capabilities in the decoder-only architecture (Section 4.1). We also find that the Adaptation module enhances both supervised and zero-shot translation performance.[8] On the other hand, InstruCL significantly boosts zero-shot capability, though there is a degradation in supervised translation performance. Additionally, with the Adaptation module implemented, the degree of degradation in supervised performance is reduced.

Moreover, the prefix decoder-only architecture achieves the highest COMET score on OPUS-100, though, it remains weaker on BERTScore compared to TDO, where both two metrics are based on semantics. This phenomenon can be explained by the target-off ratio, in which models with decoder-only architecture still have a high target-off ratio with biasing towards English primarily (Chen et al., 2023) to hamper the evaluation of COMET by considering the source sentence at the same time.

5.4 Results: Fine-tuning

Table 2 shows the experimental results by fine-tuning the pre-trained models, which shows a similar tendency to Table 1 in general. First, since we initialize the model using parameters from the decoder, the training processes for the encoder-decoder, decoder-only, and TDO architectures are relatively fair. Thus, we can conclude

[8] Appendix K shows the improvement is not because of increased parameters.

		BLEU ↑			chrF++ ↑			BERTScore ↑			COMET ↑			off ↓
		en→	→en	zero	en→	→en	zero	en→	→en	zero	en→	→en	zero	zero
M2M 418M	Enc-Dec	26.59	31.62	15.73	46.79	54.07	36.25	84.48	94.02	80.12	82.39	81.30	75.11	**3.24**
	Dec-only	25.72	30.06	14.67	45.88	52.52	34.51	84.12	93.70	79.45	81.61	79.89	73.33	3.51
	TDO	26.63	**32.44**	15.96	46.90	54.80	36.56	84.49	94.15	80.28	82.31	81.80	75.45	**3.24**
	+Adap.	**26.87**	31.93	16.12	**47.08**	54.21	36.73	**84.58**	94.08	80.35	**82.62**	81.54	75.80	3.31
	+CL	26.61	32.34	16.01	47.03	**55.07**	**36.87**	84.51	**94.16**	80.37	82.29	**81.82**	75.70	3.31
	+Adap.,+CL	26.75	31.83	**16.20**	46.98	54.09	36.82	84.56	94.07	**80.41**	82.56	81.52	**75.95**	3.30
NLLB 600M	Enc-Dec	26.39	32.04	15.44	46.90	54.51	36.09	84.46	94.07	79.96	81.98	81.16	74.05	3.42
	Dec-only	26.35	30.20	14.69	46.36	51.96	34.16	84.35	93.72	79.45	**82.20**	79.94	73.62	3.63
	TDO	25.82	32.15	15.48	46.42	54.76	36.35	84.30	94.10	80.09	81.34	81.28	74.17	**3.28**
	+Adap.	**26.60**	**32.47**	15.82	**47.04**	**54.83**	**36.62**	**84.54**	**94.15**	80.23	82.08	**81.48**	74.89	3.41
	+CL	25.87	32.29	15.48	46.44	54.71	36.21	84.31	94.11	80.09	81.43	81.27	74.18	3.47
	+Adap.,+CL	26.58	32.37	**15.85**	46.94	54.69	36.52	84.52	94.14	**80.24**	82.12	81.44	**74.93**	3.36
M2M 1.2B	Enc-Dec	27.02	31.75	16.21	47.05	53.82	36.51	84.60	94.03	80.29	82.93	81.38	76.13	**3.20**
	Dec-only	26.47	29.99	15.40	46.47	52.01	35.10	84.36	93.72	79.83	82.51	80.21	75.33	3.46
	TDO	27.17	**31.95**	16.45	47.37	**54.66**	37.24	84.64	**94.11**	80.48	82.96	81.71	76.47	3.29
	+Adap.	27.32	31.05	16.57	**47.53**	53.76	**37.47**	84.68	93.99	**80.56**	83.11	81.29	76.72	3.31
	+CL	27.27	31.83	16.57	47.32	54.42	37.08	84.67	**94.11**	80.54	83.04	**81.75**	76.72	3.32
	+Adap.,+CL	**27.41**	30.72	**16.60**	47.49	53.38	37.23	**84.70**	93.96	80.55	**83.24**	81.21	**76.88**	3.28

Table 2: Averaged scores of results in the experiments of fine-tuning. Abbreviations align with Table 2. Notably, the decoder-only and TDO architectures use Prefix masked self-attention only. The best score is in bold.

that, when compared with the decoder-only architecture, the proposed TDO architecture supports an efficient transformation from pre-trained encoder-decoder models. Secondly, when compared with the encoder-decoder models, TDO models achieve the highest scores across four metrics, reaching up to +0.39, +0.48, +0.10, and +0.31 for pairs translating to en, up to +0.82, +1.00, +0.14, and +0.52 for pairs translating from en, and up to +0.47, +0.96, +0.29, and +0.88 for zero-shot pairs. TDO models also show an improvement in the off-target ratio compared to the decoder-only models. Moreover, we observe that InstruCL does not show significant improvements in the case of NLLB-600M, whereas it remains effective in the two M2M cases. This may be attributed to that NLLB supports 205 languages, compared to 100 languages of M2M, implying a denser representational space that affects the effectiveness of InstruCL in aligning representations across languages.

6 Discussion

6.1 Representation Analysis

The limitation of the decoder-only architecture in MNMT is due to the lack of language transfer, which is shown in Figure 1b. To verify whether our proposed methods can address this issue, we analyze the layer-wise sentence representations of five models trained on TED-19: (i) a prefix decoder-only model with $N = 6$; (ii) a TDO model with $M = 6$; (iii) a TDO model with Adaption modules; (iv) a TDO model with InstrucCL; (v) a TDO model with Adaption modules and InstrucCL.

As illustrated in Figure 4, the representation of

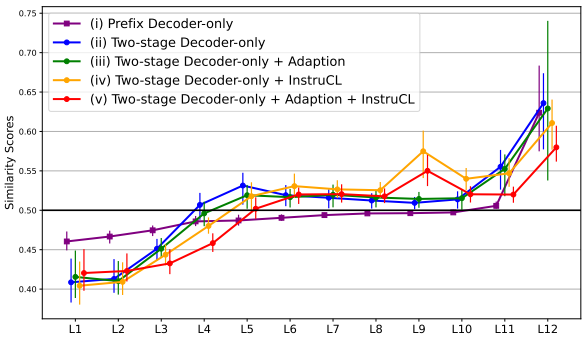

Figure 4: Illustration of linguistic preference, which follows Figure 1b. All cases in this figure use the Prefix manner for the masked self-attention mechanism. The marker of prefix decoder-only is square, and our proposed methods are round. The x-axis is the index of layers, and the vertical line indicates the value range.

(i) only exhibits a preference for the target language in the last two layers. However, (ii) shows a preference for the target language from the fourth layer, and this trend continues into the second stage. Although (iii) exhibits a more stable layer-wise trend compared to (ii), it shows significant differences in the final output across languages. Meanwhile, (iv) exhibits smaller differences across languages. Finally, (v) incorporates all the advantages of (iii) and (iv). Therefore, we can conclude that the TDO enables better language transfer by aligning different languages in the representational subspace of the target language. Meanwhile, the Adaption module and InstrucCL improve the transferability of multilingual representations.

6.2 How to balance two stages?

In Section 5, we always set M equals N to ensure a fair comparison between the TDO and the

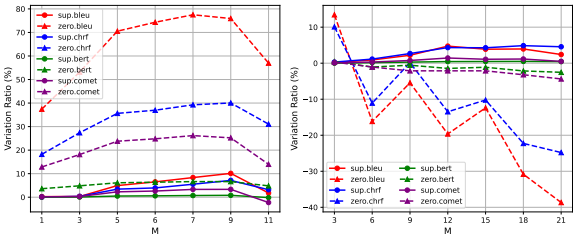

(a) TED-19 (b) OPUS-100

Figure 5: Variation in different values of M. The y-axis is the variation ratio compared to the performance of the model with prefix decoder-only architecture, and the x-axis is the value of M. The values of N are 6 and 12 in TED-19 and OPUS-100 respectively. Additionally, the line and the dotted line indicate supervised and zero-shot translations respectively.

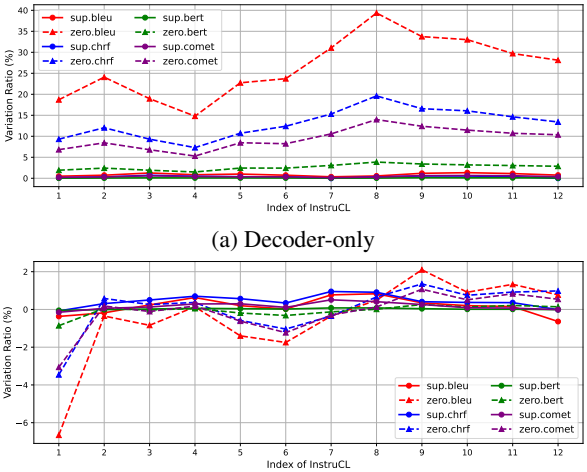

(a) Decoder-only

(b) Two-stage Decoder-only with $M = 6$

Figure 6: Variation in different layer index of InstruCL. The y-axis is the variation ratio compared to the performance of the model without InstruCL, and the x-axis is the index of the layer where InstruCL is employed.

encoder-decoder architectures. However, the balanced design is not optimal (Kasai et al., 2021; Pires et al., 2023). Thus, we test different M on TED-19 and OPUS-100 to investigate balancing two stages. As shown in Figure 5a, the performance is always improved with the increase of M on TED-19. On OPUS-100, as depicted in Figure 5b, the case with $M = 3$ achieves the best zero-shot translation scores, but there is a noticeable decline in zero-shot translation performance with the increase of M, although supervised translation scores continue to rise.

Those results align with our expectations. As shown in Table 1: 1) models with the decoder-only architecture consistently underperform compared to those with the encoder-decoder architecture in supervised translation; 2) models with the decoder-only architecture underperform in zero-shot translation on TED-19 but outperform on OPUS-100. Moreover, based on the trends in Figure 5b, we can state that the first stage enhances language transfer but at the cost of learning linguistic diversity, and the second stage benefits linguistic diversity. This statement aligns with Zhang et al. (2022) and is further proven by Table 1 where incorporating InstruCL can significantly improve the performance of zero-shot translation on OPUS-100. Thus, we conclude that the first stage is crucial in small-scale datasets, whereas the second stage becomes more significant in large-scale datasets.

6.3 How to set layer index for InstruCL?

In Section 5, we set the layer index for InstruCL to $1.5N$ to prevent the degradation of language transfer in the second stage. Given that Section 6.2 shows the different roles of the first and second stages, we test the performance of models with different layer indexes of InstruCL for the decoder-only and the TDO models. Figure 6a demonstrates that InstruCL consistently yields positive gains for the decoder-only architecture. On the other hand, Figure 6b shows a decline in the first stage but benefits in the second stage. These results indicate that InstruCL primarily affects layers that follow the decoder-only manner, namely, the second stage of TDO, which is further supported by Appendix I[9]. Moreover, another observation aligning our motivation is that an excessively high index leads to reduced gains. Therefore, we can conclude that the optimal position for implementing InstruCL is the middle layer of the second stage.

7 Conclusions

In this work, we analyzed the reasons behind the underperformance of the decoder-only architecture in MNMT, identifying the lack of language transfer capability as the primary challenge. To address this, we introduced the Two-stage Decoder-only architecture. We also proposed Instruction-level Contrastive Learning to overcome the issue from the perspective of representation optimization. We conducted experiments on two settings, i.e., training from scratch and fine-tuning, using the TED-19 and OPUS-100 datasets, and the results validate the effectiveness of our approach. Through further experiments and representation analysis, we confirm that the improvements in our methods are derived from enhanced language transfer capabilities.

[9]Appendix I shows experiments on implementing InstruCL in different architectures and datasets as a supplement.

8 Limitations

As mentioned in Section 1, this work primarily focused on addressing the challenges faced by models with a decoder-only architecture in multilingual neural machine translation (MNMT), rather than exploring how to apply large language models (LLMs), which also have the decoder-only architecture. This focus is because small models in MNMT still offer the advantages of low training and deployment costs while remaining competitive with LLMs (Zhu et al., 2023). With the increasing interest in improving multilingual translation with LLMs (Xu et al., 2024), further exploration is needed to determine whether the representation-level methods proposed in this work can be extended to LLMs. However, this is beyond the scope of the current study, as the data used to train MNMT models significantly differs from that used to train LLMs. Therefore, we leave this question for future research.

9 Ethical Considerations

All datasets and toolkits used in this work are public, common, and general in the research on multilingual neural machine translation, meanwhile, the usage of those datasets and toolkits follows the license. Moreover, this work is foundational research and is not a report of specific applications. Therefore, this work is harmless and has no ethical risks.

References

Ankur Bapna and Orhan Firat. 2019. Simple, scalable adaptation for neural machine translation. In *Proceedings of the 2019 Conference on Empirical Methods in Natural Language Processing and the 9th International Joint Conference on Natural Language Processing (EMNLP-IJCNLP)*, pages 1538–1548, Hong Kong, China. Association for Computational Linguistics.

Tom Brown, Benjamin Mann, Nick Ryder, Melanie Subbiah, Jared D Kaplan, Prafulla Dhariwal, Arvind Neelakantan, Pranav Shyam, Girish Sastry, Amanda Askell, Sandhini Agarwal, Ariel Herbert-Voss, Gretchen Krueger, Tom Henighan, Rewon Child, Aditya Ramesh, Daniel Ziegler, Jeffrey Wu, Clemens Winter, Chris Hesse, Mark Chen, Eric Sigler, Mateusz Litwin, Scott Gray, Benjamin Chess, Jack Clark, Christopher Berner, Sam McCandlish, Alec Radford, Ilya Sutskever, and Dario Amodei. 2020. Language models are few-shot learners. In *Advances in Neural Information Processing Systems*, volume 33, pages 1877–1901. Curran Associates, Inc.

Liang Chen, Shuming Ma, Dongdong Zhang, Furu Wei, and Baobao Chang. 2023. On the off-target problem of zero-shot multilingual neural machine translation. In *Findings of the Association for Computational Linguistics: ACL 2023*, pages 9542–9558, Toronto, Canada. Association for Computational Linguistics.

Alexis Conneau, Kartikay Khandelwal, Naman Goyal, Vishrav Chaudhary, Guillaume Wenzek, Francisco Guzmán, Edouard Grave, Myle Ott, Luke Zettlemoyer, and Veselin Stoyanov. 2019. Unsupervised cross-lingual representation learning at scale. *arXiv preprint arXiv:1911.02116*.

Raj Dabre, Chenhui Chu, and Anoop Kunchukuttan. 2020. A survey of multilingual neural machine translation. *ACM Comput. Surv.*, 53(5).

Jacob Devlin, Ming-Wei Chang, Kenton Lee, and Kristina Toutanova. 2018. BERT: pre-training of deep bidirectional transformers for language understanding. *CoRR*, abs/1810.04805.

Li Dong, Nan Yang, Wenhui Wang, Furu Wei, Xiaodong Liu, Yu Wang, Jianfeng Gao, Ming Zhou, and Hsiao-Wuen Hon. 2019. Unified language model pre-training for natural language understanding and generation. *Preprint*, arXiv:1905.03197.

Angela Fan, Shruti Bhosale, Holger Schwenk, Zhiyi Ma, Ahmed El-Kishky, Siddharth Goyal, Mandeep Baines, Onur Celebi, Guillaume Wenzek, Vishrav Chaudhary, Naman Goyal, Tom Birch, Vitaliy Liptchinsky, Sergey Edunov, Edouard Grave, Michael Auli, and Armand Joulin. 2020. Beyond english-centric multilingual machine translation. *Preprint*, arXiv:2010.11125.

Orhan Firat, Baskaran Sankaran, Yaser Al-onaizan, Fatos T. Yarman Vural, and Kyunghyun Cho. 2016. Zero-resource translation with multi-lingual neural machine translation. In *Proceedings of the 2016 Conference on Empirical Methods in Natural Language Processing*, pages 268–277, Austin, Texas. Association for Computational Linguistics.

Yingbo Gao, Christian Herold, Zijian Yang, and Hermann Ney. 2022. Is encoder-decoder redundant for neural machine translation? In *Proceedings of the 2nd Conference of the Asia-Pacific Chapter of the Association for Computational Linguistics and the 12th International Joint Conference on Natural Language Processing (Volume 1: Long Papers)*, pages 562–574, Online only. Association for Computational Linguistics.

Naman Goyal, Jingfei Du, Myle Ott, Giri Anantharaman, and Alexis Conneau. 2021. Larger-scale transformers for multilingual masked language modeling. *arXiv preprint arXiv:2105.00572*.

Naman Goyal, Cynthia Gao, Vishrav Chaudhary, Peng-Jen Chen, Guillaume Wenzek, Da Ju, Sanjana Krishnan, Marc'Aurelio Ranzato, Francisco Guzmán, and Angela Fan. 2022. The Flores-101 evaluation

benchmark for low-resource and multilingual machine translation. *Transactions of the Association for Computational Linguistics*, 10:522–538.

Jiatao Gu, Yong Wang, Kyunghyun Cho, and Victor O.K. Li. 2019. Improved zero-shot neural machine translation via ignoring spurious correlations. In *Proceedings of the 57th Annual Meeting of the Association for Computational Linguistics*, pages 1258–1268, Florence, Italy. Association for Computational Linguistics.

Ashish Jaiswal, Ashwin Ramesh Babu, Mohammad Zaki Zadeh, Debapriya Banerjee, and Fillia Makedon. 2021. A survey on contrastive self-supervised learning. *Preprint*, arXiv:2011.00362.

Melvin Johnson, Mike Schuster, Quoc V. Le, Maxim Krikun, Yonghui Wu, Zhifeng Chen, Nikhil Thorat, Fernanda Viégas, Martin Wattenberg, Greg Corrado, Macduff Hughes, and Jeffrey Dean. 2017. Google's multilingual neural machine translation system: Enabling zero-shot translation. *Transactions of the Association for Computational Linguistics*, 5:339–351.

Jungo Kasai, Nikolaos Pappas, Hao Peng, James Cross, and Noah Smith. 2021. Deep encoder, shallow decoder: Reevaluating non-autoregressive machine translation. In *International Conference on Learning Representations*.

Diederik P. Kingma and Jimmy Ba. 2017. Adam: A method for stochastic optimization. *Preprint*, arXiv:1412.6980.

Philipp Koehn. 2004. Statistical significance tests for machine translation evaluation. In *Proceedings of the 2004 Conference on Empirical Methods in Natural Language Processing*, pages 388–395, Barcelona, Spain. Association for Computational Linguistics.

Taku Kudo and John Richardson. 2018. SentencePiece: A simple and language independent subword tokenizer and detokenizer for neural text processing. In *Proceedings of the 2018 Conference on Empirical Methods in Natural Language Processing: System Demonstrations*, pages 66–71, Brussels, Belgium. Association for Computational Linguistics.

Sneha Kudugunta, Ankur Bapna, Isaac Caswell, and Orhan Firat. 2019. Investigating multilingual NMT representations at scale. In *Proceedings of the 2019 Conference on Empirical Methods in Natural Language Processing and the 9th International Joint Conference on Natural Language Processing (EMNLP-IJCNLP)*, pages 1565–1575, Hong Kong, China. Association for Computational Linguistics.

Yinhan Liu, Jiatao Gu, Naman Goyal, Xian Li, Sergey Edunov, Marjan Ghazvininejad, Mike Lewis, and Luke Zettlemoyer. 2020. Multilingual denoising pre-training for neural machine translation. *Preprint*, arXiv:2001.08210.

Myle Ott, Sergey Edunov, Alexei Baevski, Angela Fan, Sam Gross, Nathan Ng, David Grangier, and Michael Auli. 2019. fairseq: A fast, extensible toolkit for sequence modeling. In *Proceedings of the 2019 Conference of the North American Chapter of the Association for Computational Linguistics (Demonstrations)*, pages 48–53, Minneapolis, Minnesota. Association for Computational Linguistics.

Xiao Pan, Mingxuan Wang, Liwei Wu, and Lei Li. 2021. Contrastive learning for many-to-many multilingual neural machine translation. In *Proceedings of the 59th Annual Meeting of the Association for Computational Linguistics and the 11th International Joint Conference on Natural Language Processing (Volume 1: Long Papers)*, pages 244–258, Online. Association for Computational Linguistics.

Kishore Papineni, Salim Roukos, Todd Ward, and Wei-Jing Zhu. 2002. Bleu: a method for automatic evaluation of machine translation. In *Proceedings of the 40th Annual Meeting of the Association for Computational Linguistics*, pages 311–318, Philadelphia, Pennsylvania, USA. Association for Computational Linguistics.

Telmo Pires, Robin Schmidt, Yi-Hsiu Liao, and Stephan Peitz. 2023. Learning language-specific layers for multilingual machine translation. In *Proceedings of the 61st Annual Meeting of the Association for Computational Linguistics (Volume 1: Long Papers)*, pages 14767–14783, Toronto, Canada. Association for Computational Linguistics.

Maja Popović. 2015. chrF: character n-gram F-score for automatic MT evaluation. In *Proceedings of the Tenth Workshop on Statistical Machine Translation*, pages 392–395, Lisbon, Portugal. Association for Computational Linguistics.

Maja Popović. 2017. chrF++: words helping character n-grams. In *Proceedings of the Second Conference on Machine Translation*, pages 612–618, Copenhagen, Denmark. Association for Computational Linguistics.

Matt Post. 2018. A call for clarity in reporting BLEU scores. In *Proceedings of the Third Conference on Machine Translation: Research Papers*, pages 186–191, Brussels, Belgium. Association for Computational Linguistics.

Zhi Qu, Chenchen Ding, and Taro Watanabe. 2024. Languages transferred within the encoder: On representation transfer in zero-shot multilingual translation. *Preprint*, arXiv:2406.08092.

Zhi Qu and Taro Watanabe. 2022. Adapting to non-centered languages for zero-shot multilingual translation. In *Proceedings of the 29th International Conference on Computational Linguistics*, pages 5251–5265, Gyeongju, Republic of Korea. International Committee on Computational Linguistics.

Alec Radford, Karthik Narasimhan, Tim Salimans, Ilya Sutskever, et al. 2018. Improving language understanding by generative pre-training.

Colin Raffel, Noam Shazeer, Adam Roberts, Katherine Lee, Sharan Narang, Michael Matena, Yanqi Zhou, Wei Li, and Peter J. Liu. 2023. Exploring the limits of transfer learning with a unified text-to-text transformer. *Preprint*, arXiv:1910.10683.

Maithra Raghu, Justin Gilmer, Jason Yosinski, and Jascha Sohl-Dickstein. 2017. Svcca: Singular vector canonical correlation analysis for deep learning dynamics and interpretability. In *Proceedings of the 31st International Conference on Neural Information Processing Systems*, NIPS'17, page 6078–6087, Red Hook, NY, USA. Curran Associates Inc.

Ricardo Rei, José G. C. de Souza, Duarte Alves, Chrysoula Zerva, Ana C Farinha, Taisiya Glushkova, Alon Lavie, Luisa Coheur, and André F. T. Martins. 2022. COMET-22: Unbabel-IST 2022 submission for the metrics shared task. In *Proceedings of the Seventh Conference on Machine Translation (WMT)*, pages 578–585, Abu Dhabi, United Arab Emirates (Hybrid). Association for Computational Linguistics.

Ricardo Rei, Craig Stewart, Ana C Farinha, and Alon Lavie. 2020. COMET: A neural framework for MT evaluation. In *Proceedings of the 2020 Conference on Empirical Methods in Natural Language Processing (EMNLP)*, pages 2685–2702, Online. Association for Computational Linguistics.

David Stap, Vlad Niculae, and Christof Monz. 2023. Viewing knowledge transfer in multilingual machine translation through a representational lens. In *Findings of the Association for Computational Linguistics: EMNLP 2023*, pages 14973–14987, Singapore. Association for Computational Linguistics.

Shaomu Tan and Christof Monz. 2023. Towards a better understanding of variations in zero-shot neural machine translation performance. In *Proceedings of the 2023 Conference on Empirical Methods in Natural Language Processing*, pages 13553–13568, Singapore. Association for Computational Linguistics.

NLLB Team, Marta R. Costa-jussà, James Cross, Onur Çelebi, Maha Elbayad, Kenneth Heafield, Kevin Heffernan, Elahe Kalbassi, Janice Lam, Daniel Licht, Jean Maillard, Anna Sun, Skyler Wang, Guillaume Wenzek, Al Youngblood, Bapi Akula, Loic Barrault, Gabriel Mejia Gonzalez, Prangthip Hansanti, John Hoffman, Semarley Jarrett, Kaushik Ram Sadagopan, Dirk Rowe, Shannon Spruit, Chau Tran, Pierre Andrews, Necip Fazil Ayan, Shruti Bhosale, Sergey Edunov, Angela Fan, Cynthia Gao, Vedanuj Goswami, Francisco Guzmán, Philipp Koehn, Alexandre Mourachko, Christophe Ropers, Safiyyah Saleem, Holger Schwenk, and Jeff Wang. 2022. No language left behind: Scaling human-centered machine translation. *Preprint*, arXiv:2207.04672.

Ashish Vaswani, Noam Shazeer, Niki Parmar, Jakob Uszkoreit, Llion Jones, Aidan N Gomez, Ł ukasz Kaiser, and Illia Polosukhin. 2017. Attention is all you need. In *Advances in Neural Information Processing Systems*, volume 30. Curran Associates, Inc.

Thomas Wang, Adam Roberts, Daniel Hesslow, Teven Le Scao, Hyung Won Chung, Iz Beltagy, Julien Launay, and Colin Raffel. 2022. What language model architecture and pretraining objective work best for zero-shot generalization? *Preprint*, arXiv:2204.05832.

Liwei Wu, Shanbo Cheng, Mingxuan Wang, and Lei Li. 2021. Language tags matter for zero-shot neural machine translation. In *Findings of the Association for Computational Linguistics: ACL-IJCNLP 2021*, pages 3001–3007, Online. Association for Computational Linguistics.

Haoran Xu, Young Jin Kim, Amr Sharaf, and Hany Hassan Awadalla. 2024. A paradigm shift in machine translation: Boosting translation performance of large language models. In *The Twelfth International Conference on Learning Representations*.

Wen Yang, Chong Li, Jiajun Zhang, and Chengqing Zong. 2023. Bigtranslate: Augmenting large language models with multilingual translation capability over 100 languages. *Preprint*, arXiv:2305.18098.

Yilin Yang, Akiko Eriguchi, Alexandre Muzio, Prasad Tadepalli, Stefan Lee, and Hany Hassan. 2021. Improving multilingual translation by representation and gradient regularization. In *Proceedings of the 2021 Conference on Empirical Methods in Natural Language Processing*, pages 7266–7279, Online and Punta Cana, Dominican Republic. Association for Computational Linguistics.

Qi Ye, Sachan Devendra, Felix Matthieu, Padmanabhan Sarguna, and Neubig Graham. 2018. When and why are pre-trained word embeddings useful for neural machine translation. In *HLT-NAACL*.

Biao Zhang, Behrooz Ghorbani, Ankur Bapna, Yong Cheng, Xavier Garcia, Jonathan Shen, and Orhan Firat. 2022. Examining scaling and transfer of language model architectures for machine translation. In *Proceedings of the 39th International Conference on Machine Learning*, volume 162 of *Proceedings of Machine Learning Research*, pages 26176–26192. PMLR.

Biao Zhang, Philip Williams, Ivan Titov, and Rico Sennrich. 2020a. Improving massively multilingual neural machine translation and zero-shot translation. In *Proceedings of the 58th Annual Meeting of the Association for Computational Linguistics*, pages 1628–1639, Online. Association for Computational Linguistics.

Shaolei Zhang, Qingkai Fang, Zhuocheng Zhang, Zhengrui Ma, Yan Zhou, Langlin Huang, Mengyu Bu, Shangtong Gui, Yunji Chen, Xilin Chen, and Yang Feng. 2023. Bayling: Bridging cross-lingual alignment and instruction following through interactive translation for large language models. *Preprint*, arXiv:2306.10968.

Tianyi Zhang, Varsha Kishore, Felix Wu, Kilian Q. Weinberger, and Yoav Artzi. 2020b. Bertscore:

Evaluating text generation with bert. *Preprint*, arXiv:1904.09675.

Wenhao Zhu, Hongyi Liu, Qingxiu Dong, Jingjing Xu, Shujian Huang, Lingpeng Kong, Jiajun Chen, and Lei Li. 2023. Multilingual machine translation with large language models: Empirical results and analysis. *Preprint*, arXiv:2304.04675.

A Introduction of Illustrating Linguistic Preference

Overview In this work, we only quantify the language features of the sentence representation by the similarity scores, although the analysis of Qu et al. (2024) further quantified the semantic features of representations. Specifically, the score presents whether the sentence representations at a certain state exhibit more features related to the target language or more features related to the source language.

Setup First, quantifying the language features of the sentence representation requires a semantically parallel dataset. Therefore, we conduct analysis experiments on TED-19, which provides six fully parallel languages, including `ar`, `he`, `zh`, `hr`, `vi`, and `ja`. We connect these languages to generate 30 zero-shot translation pairs, each pair consisting of 967 sentences. The model setup is consistent with our main experiments (Section 5).

Computing the similarity score First, we follow the process of Qu et al. (2024) to measure representation similarity in MNMT, employing singular value canonical correlation analysis (Raghu et al., 2017). As the definition in Section 3, we obtain the token-wise hidden representations of the source sentence, i.e. $\mathbf{H}$, from a translation pair. Notably, for a decoder-only model, we cut out the source part, namely, $|\mathbf{H}|$ is always $I+1$. Then, we derive the sentence-level representation $\overline{\boldsymbol{h}}$ using average pooling $\overline{\boldsymbol{h}} = \frac{\sum_{i=1}^{q} \boldsymbol{h}_i}{q}$. Given $\mathbf{H}^a$ and $\mathbf{H}^b$ derived from two sentences, we first perform singular value decomposition on $\overline{\boldsymbol{h}}^a$ and $\overline{\boldsymbol{h}}^b$ to obtain subspace representations $\overline{\boldsymbol{h}}^a \in \mathbb{R}^{d^a}$ and $\overline{\boldsymbol{h}}^b \in \mathbb{R}^{d^b}$. Then we perform canonical correlation analysis to determine $\mathbf{W}^a \in \mathbb{R}^{d' \times d^a}$ and $\mathbf{W}^b \in \mathbb{R}^{d' \times d^b}$. Formally, we compute correlation ρ between $\overline{\boldsymbol{h}}^a$ and $\overline{\boldsymbol{h}}^b$ as

$$\rho = \frac{\langle \mathbf{W}^a \overline{\boldsymbol{h}}^a, \mathbf{W}^b \overline{\boldsymbol{h}}^b \rangle}{\|\mathbf{W}^a \overline{\boldsymbol{h}}^a\| \|\mathbf{W}^b \overline{\boldsymbol{h}}^b\|}, \tag{10}$$

where $\langle \cdot, \cdot \rangle$ indicates the inner product. We use ρ to represent the similarity of two sentences.

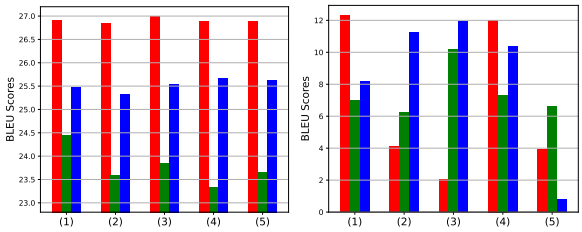

(a) supervised (b) zero-shot

Figure 7: Averaged BLEU scores in different architectures. The palette follows Figure 1, i.e., red is encoder-decoder, green is causal decoder-only, and blue is prefix decoder-only.

Subsequently, we get the similarity $\rho_{\boldsymbol{x}}$ between $(l_{\boldsymbol{y}}, \boldsymbol{x}, \boldsymbol{y})$ and $(l_{\boldsymbol{x}}, \boldsymbol{x}, \boldsymbol{x})$ and the similarity $\rho_{\boldsymbol{y}}$ between $(l_{\boldsymbol{y}}, \boldsymbol{x}, \boldsymbol{y})$ and $(l_{\boldsymbol{y}}, \boldsymbol{y}, \boldsymbol{y})$, respectively. Therefore, a similarity score of linguistic preference is computed as follows:

$$s_{(l_{\boldsymbol{y}}, \boldsymbol{x}, \boldsymbol{y})} = \frac{\rho_{\boldsymbol{y}}}{\rho_{\boldsymbol{y}} + \rho_{\boldsymbol{x}}}, \tag{11}$$

where $s_{(l_{\boldsymbol{y}}, \boldsymbol{x}, \boldsymbol{y})}$ is the similarity score for the given translation pair. Finally, we compute the set-level score by taking the average scores of all sentences over the test set.

Meaning of the similarity score Equation 11 simply compares the importance of source information and target information in the representation. Therefore, a value higher than 0.5 means the representation prefers the target language, otherwise the representation prefers the source language. Moreover, the value reflects the degree of linguistic preference, for example, compared to 0.6, 0.7 means the representation presents much more features of the target language or fewer features of the source language. In addition, we also denote the highest and lowest values by the vertical lines on each point in Figures 1b and 4 to show the value range, which can present stability. Finally, we can find that models with decoder-only architecture cannot align the representation of the source tokens in the representational subspace of the target language, and they try to align source and target languages to be a language-agnostic state.

B Comparison between Different Instruction Strategies in MNMT

MNMT is sensitive to the strategy of translation instruction (Wu et al., 2021). We summarize the possible strategies as follows: (1) Adding a language tag specified to the target language at the beginning

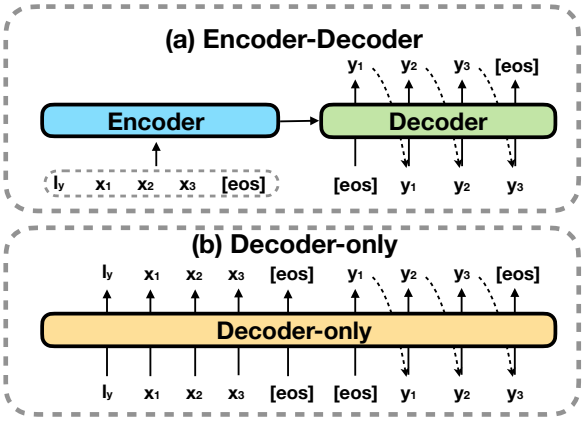

Figure 8: Illustration of input and output forms in MNMT. Subfigures are for the encoder-decoder architecture and the decoder-only architecture, respectively. [eos] is a special token, which means the end of a sentence and is regarded as a token of $\boldsymbol{x}$ and $\boldsymbol{y}$.

of source tokens; (2) Adding a language tag specified to the target language at the beginning of target tokens; (3) Based on the (2), using the language tag to replace the [eos] token, which is used to be the trigger of inference; (4) Adding two language tag specified to the target language at the beginning of source tokens and the beginning of target tokens, simultaneously; (5) Adding a language tag specified to the source language and a language tag specified to the target language at the beginning of source tokens and target tokens, respectively. Then, we conduct preliminary experiments on three architectures: encoder-decoder, causal decoder-only, and prefix decoder-only, to support the validity of using approach (1). As shown in Figure 7, the performance of encoder-decoder architecture meets the analysis of Wu et al. (2021). However, a language tag at the beginning of target tokens, i.e., (2), (3), and (4), is more beneficial for the zero-shot capability in Decoder-only architecture. Considering that (1) also benefits decoder-only architectures in the supervised translation, using (1) in this work is reasonable.

C Different Input and Output Forms

Figure 8 illustrates input and output forms for two architectures involved in this work. Initially, within the encoder-decoder architecture, the encoder receives parallel input from source tokens, including $l_{\boldsymbol{y}}$, $\boldsymbol{x}$, and a special token [eos]. As a supplement of Section 3.2, for the $I+1$ tokens feeding to the encoder, $l_{\boldsymbol{y}}$ is the first token and corresponds to the $\boldsymbol{h}_1$, then, each index of $\boldsymbol{x}$ is shifted, namely, $\boldsymbol{x}$ corresponds to $\{\boldsymbol{h}_2, ..., \boldsymbol{h}_{I+1}\}$. Furthermore, the input

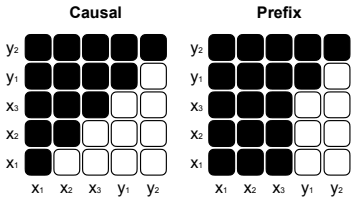

Figure 9: Different manners of the masked self-attention mechanism in the decoder-only architectures. Black blocks mean visible and white blocks mean masked. Thus, source tokens are masked in the causal decoder-only while are visible in the prefix decoder-only.

of the decoder is shifted. Specifically, in training, [eos] is placed at the beginning of the target tokens, and the output at each position always points to the token in the next position; in inference, [eos] serves as the trigger, and the model would generate the next token step by step until the predicted token is [eos]. Finally, the output of the encoder-decoder architecture only includes target tokens, i.e., $\boldsymbol{y}$. On the other hand, the decoder-only architecture combines source tokens and target tokens as the input. In this work, we follow Zhang et al. (2022); Gao et al. (2022) to employ MNMT loss instead of language modeling loss, namely, cutting off the source tokens and saving the target tokens only in the ouput,

D Attention Mechanisms of Decoder-Only Architectures

As illustrated in Figure 9, the causal attention mechanism in the decoder-only architecture treats source and target tokens equally, meaning that each token is influenced solely by preceding tokens and itself. In contrast, the prefix attention mechanism maintains bi-directional attention for source tokens where source tokens are influenced by each other, while target tokens use mono-directional attention, meaning they are influenced only by prior tokens and themselves.

E Estimation of Parameters

We follow the notation in Section 5.2, that is, d is the dimension of the model and the inner size of FFN is $4d$. Therefore, each attention mechanism has $4d^2$ parameters because there are 4 matrices with dimensions of $d \times d$, and each FFN has $8d^2$ parameters (Vaswani et al., 2017). Then, all layers have the structure illustrated in Figure 2. Given $N=1$, the model with encoder-decoder architecture has $28d^2$ parameters and the model

with Decoder-only architecture has $24d^2$ parameters. Thus, considering the fixed parameters of normalization modules and embedding layer, Decoder-only architecture is implemented with around 10% fewer parameters than encoder-decoder architecture.

F Detailed Information of Datasets

First, the language codes used in our descriptions adhere to ISO 639-1[10]. As described in Section 5.1, the first dataset is TED-19 (Qu et al., 2024), a subset of TED Talks (Ye et al., 2018) containing 6.5 million instances across 19 languages from various language families. This dataset includes 32 supervised translation pairs and 306 zero-shot translation pairs. Detailed information about TED-19 is provided in Table 7. The second dataset is the revised version of OPUS-100 (Zhang et al., 2020a; Yang et al., 2021), which includes 95 languages and a total of 92 million instances. Notably, the zero-shot translation in OPUS-100 involves only six languages (`ar`, `nl`, `de`, `zh`, `ru`, and `fr`), resulting in 30 translation pairs. Additionally, we further cleaned the dataset by removing noisy instances containing unreadable characters, even though Yang et al. (2021) had already removed repetitions from the original OPUS-100 dataset (Zhang et al., 2020a). Detailed information about OPUS-100 can be found in Table 8. Generally, each pair of validation and test sets in these two datasets contains 2,000 instances, though several pairs in OPUS-100 have fewer instances. Finally, we used SentencePiece (Kudo and Richardson, 2018) to generate the vocabulary for training, with the vocabulary size set to 50,000 for TED-19 and 64,000 for OPUS-100.

G Evaluation Metrics

First, SacreBLEU (Post, 2018), an implementation of BLEU (Papineni et al., 2002), measures the lexical overlap between generated translations and reference translations. chrF++ evaluates overlap at the character level and accounts for a balance between precision and recall. These two metrics can corroborate each other's results. On the other hand, BERTScore[11] (Zhang et al., 2020b) measures the similarity between generated translations and references at the representation level. COMET[12] (Rei et al., 2020) also evaluates representational similarity, with an additional emphasis on the source text for enhanced semantic relevance. Intuitively, BERTScore may penalize instances that do not translate into the expected target language, while COMET is more sensitive to semantic relevance. To validate this intuition, we employ *fasttext-langdetect*[13] to measure the target-off ratio on zero-shot pairs, i.e., the ratio of cases where the source sentence is not translated into the correct target language, as a secondary metric. Notably, it is considered secondary because the testing tools are not entirely accurate, particularly when recognizing low-resource languages, as they rely on language-specific tokens. Finally, to show whether the improvements of zero-shot translations brought by proposed methods are significant, we also conduct the statistical significance testing (Koehn, 2004) using paired bootstrap resampling with 1,000 iterations and 0.5 resampling ratios, consequently, the case of $p < 0.1$ means that the difference is significant.

H Detailed Model Settings

We implement models by Fairseq (Ott et al., 2019), an open-source toolkit. First of all, in this work, we apply independent sinusoidal positional embeddings for source tokens and target tokens (Vaswani et al., 2017) for the input of the decoder-only architecture. Notably, the estimation of parameters in modeling is introduced in Appendix E.

Model settings of training from scratch In the case of training from scratch on TED-19, we set N to 6, d to 512, inner size of FFN to $4d$. Thus, the model with an encoder-decoder architecture has 70 million parameters, while the model with a decoder-only architecture has 63 million parameters. Moreover, the FFN in the adaptation module matches the dimensions of the FFN in the main part, so in this case, the model has 67 million parameters. In the training, we set the learning rate to 0.0005 and the model is trained for 30 epochs on eight NVIDIA V100 GPUs with a batch size of 4,000 per GPU to ensure full convergence. Moreover, we set the head number of the attention mechanism to 8, the dropout rate to 0.1, label smoothing to

[10] https://www.loc.gov/standards/iso639-2/php/code_list.php

[11] For BERTScore, en is computed using *xlmr.large* (Conneau et al., 2019; Goyal et al., 2021), while other languages are computed using *bert-base-multilingual-cased* (Devlin et al., 2018).

[12] All COMET scores are computed using *Unbabel/wmt22-comet-da* (Rei et al., 2022).

[13] https://pypi.org/project/fasttext-langdetect

					BLEU ↑			chrF++ ↑			BERTScore ↑			COMET ↑		
		#enc	#dec	idx.	en→	→en	zero	en→	→en	zero	en→	→en	zero	en→	→en	zero
TED d =512	Enc-Dec	6	6	-	25.46	28.31	12.32	45.96	50.86	32.13	84.10	93.37	78.03	80.49	78.15	67.26
		6	6	6	24.92	28.39	12.96	45.56	50.97	33.42	83.94	93.68	79.10	79.99	78.21	70.37
	Dec-only	0	12	-	24.00	26.97	8.18	44.49	48.93	25.35	83.54	92.97	74.52	78.46	76.10	56.74
		0	12	6	24.16	27.18	10.12	44.61	49.11	28.49	83.63	93.01	76.32	78.80	76.30	61.41
		0	12	9	24.26	27.31	10.94	44.69	49.24	29.55	83.69	93.05	77.05	79.08	76.45	63.77
	TDO	0	12	-	25.53	28.76	14.26	46.01	51.09	34.72	84.13	93.41	79.27	80.43	78.18	70.82
		0	12	6	25.46	**29.02**	14.06	45.98	51.44	34.38	84.10	93.48	79.15	80.47	78.54	70.51
		0	12	9	**25.62**	28.94	**14.70**	**46.15**	**51.46**	**35.34**	**84.15**	**93.47**	**79.57**	**80.55**	**78.55**	**71.94**
OPUS d =512	Enc-Dec	12	12	-	**25.18**	29.79	5.13	**44.75**	48.40	12.95	**82.98**	92.33	72.44	**76.59**	76.21	58.51
		12	12	12	24.98	29.61	6.56	44.65	48.30	15.49	82.97	92.34	73.45	76.46	76.23	59.61
	Dec-only	0	24	-	23.96	28.41	6.62	42.98	47.22	15.36	82.47	92.06	73.57	75.48	75.34	**59.56**
		0	24	12	24.22	28.26	6.99	43.23	46.83	15.98	82.49	92.04	73.66	75.55	74.94	59.42
		0	24	18	23.98	28.22	6.73	43.18	46.80	16.17	82.52	92.07	73.67	75.60	75.12	59.37
	TDO	0	24	-	24.88	**29.97**	5.32	44.72	**49.39**	13.29	82.91	**92.41**	72.50	76.26	**76.73**	58.30
		0	24	12	24.61	29.37	6.46	44.68	48.72	15.14	82.87	92.37	73.30	76.16	76.21	59.41
		0	24	18	24.35	29.52	**7.93**	44.44	48.74	**18.65**	82.84	92.37	**73.97**	75.93	76.23	58.71
OPUS d =1024	Enc-Dec	6	6	-	27.71	**31.60**	6.95	46.84	50.31	15.89	83.55	92.62	74.12	**78.10**	77.58	59.99
		6	6	6	**27.74**	31.52	7.75	**46.92**	49.91	18.06	**83.56**	**92.66**	74.44	78.07	77.69	60.43
	Dec-only	0	12	-	26.79	30.42	8.15	45.48	48.92	17.65	83.21	92.37	74.17	77.53	76.69	**62.32**
		0	12	6	26.87	30.72	8.47	45.58	49.18	17.78	83.53	92.51	74.38	77.74	77.82	61.61
		0	12	9	26.72	30.09	8.42	45.34	48.52	17.33	83.16	91.83	74.23	77.31	76.61	61.55
	TDO	0	12	-	27.22	31.58	7.06	46.54	**50.59**	15.96	83.44	92.64	73.78	77.68	**77.89**	60.60
		0	12	6	26.72	31.05	7.43	45.49	49.54	16.25	83.19	92.40	74.00	77.45	77.49	61.89
		0	12	9	27.12	31.49	**9.28**	46.55	50.23	**21.33**	83.50	92.65	**75.04**	77.63	77.64	60.84

Table 3: Averaged scores of results in experiments of training from scratch and verifying InstruCL across different architectures. Both the decoder-only and TDO architectures adopt the prefix attention mechanism. All terms, settings, and abbreviations follow the Table 1. Moreover, #enc, #dec, and idx. indicate the number of encoder layers, the number of decoder layers, and the layer index where to implement InstruCL, respectively. In addition, the placeholder (-) in the collum of idx. means that InstruCL is not implemented in this row. The best score in each column and block is in bold.

0.1, and weight decay to 0.0001. We also employ Adam (Kingma and Ba, 2017) as our optimizer and set *share-all-embeddings* of Fairseq. We evaluate by averaging the top-5 best checkpoints selected based on validation loss. In the case of training from scratch on OPUS-100, we first increase N to 12, resulting in parameter counts of 121 million, 108 million, and 113 million, respectively. In the training, we set the number of gradient accumulation steps to 16 to increase the batch size and train for 50,000 steps with a learning rate of 0.0007. We also consider a wider model where N is 6, d is 1024, and the head number of the attention mechanism is 16, resulting in parameter counts of 242 million, 217 million, and 234 million, respectively. When, we additionally set an attention dropout to 0.05 and reduce the learning rate to 0.0005 for a stable gradient. Moreover, we reduce the batch size per GPU to 2,000, set the number of gradient accumulation steps to 32, and train for 100,000 steps due to GPU memory constraints. For two cases of OPUS-100, we test the checkpoint with the best validation loss. Additionally, in training on OPUS-100, we set *encoder-normalize-before* and *decoder-normalize-before* in Fairseq and reduce the weight decay to 0, which lead to a quick convergence in a complex data condition (Liu et al., 2020; Fan et al., 2020; Team et al., 2022).

Model settings of fine-tuning In the model settings of fine-tuning, M2M-418M has 12 layers for encoder and decoder, respectively, where d of M2M-418M is 1024, and the inner size of FFN is 4096, based on the description in Section 5.2, we set N to 6, resulting in parameter counts of 307 million, 282 million, and 299 million, respectively. In the training, the label smoothing is 0.2, the dropout is 0.3, the attention dropout is 0.05, and the batch size and the learning rate keep the settings of training from scratch. Then, given that NLLB-600M has the same configuration as M2M-418M but with a larger vocabulary size, the same setting of hyper-parameters leads to the count of parameters increased to 439 million, 413 million, and 430 million, respectively, and, we reduce the batch size to 2000 and set gradient accumulation to 2 for NLLB-600M because of the GPU memory constraints. In M2M-1.2B, which has 24 decoder

layers and a larger inner size of FFN compared to M2M-418M, we set N to 12, leading to parameter counts of 685 million, 635 million, and 668 million, respectively, and our experiments are conducted on four NVIDIA A6000 GPUs, and we set gradient accumulation to 2. We also reduce the learning rate to 0.0002 and the number of training epochs to 10 because of more parameters.

I The Effectiveness of InstruCL on Encoder-Decoder Architecture

As a supplementary trail for Sections 5.3 and 6.3, we conduct experiments on applying InstruCL to the encoder-decoder, the prefix decoder-only, and TDO architectures, and then compare their performances on three cases of training from scratch described in Section 5.2. The layer index where InstruCL is implemented at the TDO is $1.5N$. We also implement InstruCL for the decoder-only architecture at the same layer as a comparison. However, given that the number of encoder layers in an encoder-decoder architecture is N, InstruCl is implemented at the output of the encoder, namely, the layer index is N. Therefore, as comparison groups, we also implement InstruCL for the decoder-only and TDO architectures at the N layer.

Tabel 3 shows the experimental results. The first observation is that the encoder-decoder architecture can be gained from InstruCL due to the improved performance in all cases. Notably, the first observation is not violated from the statement in Section 6.3 that InstruCL mainly affects the layer following the decoder-only manner, because of the performance of TDO in TED-19 and OPUS-100. Specifically, considering the decoder-only architecture, first, in the TED-19, when the index is set to N, Dec-only shows a significant improvement in zero-shot translations with BLEU scores increasing by 1.94, while TDO degraded by 0.64. Second, in two cases from the OPUS-100, when the index is set to $1.5N$, TDO achieves significant improvements of 2.61 and 2.22, respectively. Third, in three cases, compared to setting the index to N, the decoder-only model showed smaller gains or even degradations when the index is set to $1.5N$, with scores increasing by 0.82, -0.26, and -0.05.

These results are consistent with our statement in Section 4.2. Specifically, the first stage of TDO overlaps with InstruCL in terms of facilitating the learning of target language representations, which explains the suboptimal performance when both are used together. Additionally, InstruCL is most effective when applied in the middle layers, which align with the decoder-only manner. On the other hand, considering the performance of the vanilla models, i.e., Enc-Dec and Dec-only, we can assert that InstruCL, which does not require additional data costs, generally benefits all architectures.

Scenario	Model	Seconds
TED	Enc-dec	22854
N=6	Dec-only	24277
d =512	TDO	**22359**
OPUS	Enc-dec	102509
N=12	Dec-only	114514
d =512	TDO	**101826**
OPUS	Enc-dec	258845
N=6	Dec-only	298344
d =1024	TDO	**247964**

Table 4: Training times of different models in three experimental settings. The smallest value is in bold.

J The Impact of Computational Complexity

Intuitively, when comparing the decoder-only architectures, TDO model exhibits lower computational complexity than the vanilla decoder-only model. This is due to the removal of the first M layers from the vanilla decoder-only model when generating target token sequences. Despite the reduced computational complexity, TDO achieves superior performance compared to the vanilla decoder-only architecture. Second, we present an empirical comparison of training times across different models. Table 4 summarizes the results, showing that TDO has the shortest training time, comparable to the encoder-decoder model.

Next, we formally estimate the computational complexity for each architecture. For simplicity, we omit the layer normalization and output projection components from the analysis. Let the model dimension be denoted by d, the inner size of the feed-forward network by $4d$, and the total number of tokens be $2n$, where n represents both the source and target tokens. The number of layers is assumed to be one encoder layer, one decoder layer, and two decoder-only layers. As shown in Table 5, the estimated FLOPs for TDO fall between those of the encoder-decoder (enc-dec) model and the vanilla decoder-only model. Specifically, the computational cost of TDO is lower than the vanilla decoder-only model but higher than the

enc-dec model. Despite this, TDO achieves significantly better performance than the decoder-only model and competitive performance with the enc-dec model.

Component or Architecture	Estimated FLOPs
multi-head self-attention	$4 \cdot n \cdot d^2 + 2 \cdot n^2 \cdot d$
feed-forward network	$8 \cdot n \cdot d^2$
encoder layer	$12 \cdot n \cdot d^2 + 2 \cdot n^2 \cdot d$
decoder layer	$12 \cdot n \cdot d^2 + 4 \cdot n^2 \cdot d$
decoder-only layer	$24 \cdot n \cdot d^2 + 8 \cdot n^2 \cdot d$
Enc-dec	$24 \cdot n \cdot d^2 + 6 \cdot n^2 \cdot d$
Dec-only	$48 \cdot n \cdot d^2 + 16 \cdot n^2 \cdot d$
TDO	$36 \cdot n \cdot d^2 + 10 \cdot n^2 \cdot d$

Table 5: Estimated FLOPs for various components and architectures.

Furthermore, the discrepancy between training time and theoretical FLOP counts can be attributed to the fact that TDO contains approximately 10% fewer parameters compared to the encoder-decoder architecture. This reduction in parameters contributes to faster training times, as discussed in Appendix K and cited in Section 4.1 of our manuscript. In conclusion, the observed improvements in model performance are not the result of increased computational complexity but rather due to the architectural design choices in the TDO model. The combination of empirical results and theoretical analysis demonstrates that TDO offers a more computationally efficient alternative to the decoder-only model, with competitive performance comparable to the encoder-decoder model.

K Adaption Modules Do Not Equal Simply Increasing Parameters

Adding adaptation modules increases the number of parameters, so it is crucial to determine whether the gains from these modules are primarily due to the increased parameters. As shown in Table 6, we directly increased the parameters of the TDO model using various strategies, ensuring that the number of parameters is comparable to or even greater than that of the TDO model with adaptation modules. The results demonstrate that the TDO model with adaptation modules outperforms in zero-shot translation and in translating supervised pairs from English to non-central languages. Notably, considering the previous point, the reason why adaptation modules do not achieve the best performance when translating from non-central languages to English can be attributed to their effectiveness in preventing overfitting of English, which dominates the multilingual representations due to most of the training data being in English (Gu et al., 2019; Qu and Watanabe, 2022). Therefore, the results in this table support our assertion that the gains from adaptation modules cannot be simply attributed to increasing parameters.

	d	d^1_{ffn}	d^2_{ffn}	en→	→en	zero
TDO+adapt.	512	2048	2048	**25.61**	28.52	**14.51**
TDO	544	2048	2048	25.55	28.28	14.22
	512	2432	2432	25.51	28.51	14.31
	512	2048	2816	25.32	27.98	13.89
	512	2816	2048	25.56	**28.95**	14.01

Table 6: Averaged BLEU scores of models with TDO architecture trained on TED-19. Abbreviations in this table follow Table 1. In addition, d^1_{ffn} is the inner size of FFN in the first stage, and d^2_{ffn} is in the second stage. The best score is in bold.

Code	Language	Family	Sub-Family	#Train	Code	Language	Family	Sub-Family	#Train
es	Spanish	Indo-European	Romance	196026	ar	Arabic	Afro-Asiatic	Semitic	214111
fr	French	Indo-European	Romance	192304	he	Hebrew	Afro-Asiatic	Semitic	211819
ro	Romanian	Indo-European	Romance	180484	ru	Russian	Indo-European	Slavic	208458
nl	Dutch	Indo-European	Germanic	183767	ko	Korean	Koreanic		205640
de	German	Indo-European	Germanic	167888	it	Italian	Indo-European	Romance	204503
pl	Polish	Indo-European	Slavic	176169	ja	Japanese	Japonic		204090
hr	Croatian	Indo-European	Slavic	122091	zh	Chinese	Sino-Tibetan	Sinitic	199855
cs	Czech	Indo-European	Slavic	103093	tr	Turkish	Turkic		182470
fa	Persian	Indo-European	Iranian	150965	vi	Vietnamese	Austroasiatic	Vietic	171995

Table 7: Detailed information of TED-19 datasets. #Train indicates the number of training instances.

Code	Language	Family	Sub-Family	#Train	Code	Language	Family	Sub-Family	#Train
fa	Persian	Indo-European	Iranian	934413	yi	Yiddish	Indo-European	Romance	1865
bn	Bengali	Indo-European	Iranian	724719	ga	Irish	Indo-European	Celtic	187967
ur	Urdu	Indo-European	Iranian	724226	br	Breton	Indo-European	Celtic	96951
si	Sinhala	Indo-European	Iranian	613702	cy	Welsh	Indo-European	Celtic	92615
hi	Hindi	Indo-European	Iranian	374472	gd	Scottish Gaelic	Indo-European	Celtic	11104
tg	Tajik	Indo-European	Iranian	183216	lt	Lithuanian	Indo-European	Baltic	797693
ne	Nepali	Indo-European	Iranian	144520	lv	Latvian	Indo-European	Baltic	779972
gu	Gujarati	Indo-European	Iranian	108564	tr	Turkish	Turkic		918838
ku	Kurdish	Indo-European	Iranian	107110	az	Azerbaijani	Turkic		237533
pa	Punjabi	Indo-European	Iranian	72160	uz	Uzbek	Turkic		148319
as	Assamese	Indo-European	Iranian	58009	tt	Tatar	Turkic		97746
mr	Marathi	Indo-European	Iranian	26117	ug	Uyghur	Turkic		71241
ps	Pashto	Indo-European	Iranian	14254	kk	Kazakh	Turkic		62227
or	Oriya	Indo-European	Iranian	13410	ky	Kyrgyz	Turkic		12724
de	German	Indo-European	Germanic	968252	tk	Turkmen	Turkic		98
nl	Dutch	Indo-European	Germanic	936611	ar	Arabic	Afro-Asiatic	Semitic	959868
sv	Swedish	Indo-European	Germanic	916259	he	Hebrew	Afro-Asiatic	Semitic	913493
no	Norwegian	Indo-European	Germanic	914187	mt	Maltese	Afro-Asiatic	Semitic	672134
da	Danish	Indo-European	Germanic	911156	ha	Hausa	Afro-Asiatic	Chadic	91869
is	Icelandic	Indo-European	Germanic	813820	am	Amharic	Afro-Asiatic	Semitic	64369
nn	Norwegian Nynorsk	Indo-European	Germanic	172187	el	Greek	Indo-European	Hellenic	932811
af	Afrikaans	Indo-European	Germanic	146600	sq	Albanian	Indo-European	Albanian	855095
nb	Norwegian Bokmål	Indo-European	Germanic	128374	ml	Malayalam	Dravidian		633920
fy	Frisian	Indo-European	Germanic	42372	ta	Tamil	Dravidian		184699
li	Limburgish	Indo-European	Germanic	3331	te	Telugu	Dravidian		37792
ru	Russian	Indo-European	Slavic	951611	kn	Kannada	Dravidian		13777
sr	Serbian	Indo-European	Slavic	935342	xh	Xhosa	Niger-Congo	Bantu	231708
hr	Croatian	Indo-European	Slavic	927541	rw	Kinyarwanda	Niger-Congo	Bantu	62159
pl	Polish	Indo-European	Slavic	926940	zu	Zulu	Niger-Congo	Bantu	6834
bg	Bulgarian	Indo-European	Slavic	925647	ig	Igbo	Niger-Congo	Volta-Niger	691
cs	Czech	Indo-European	Slavic	924282	fi	Finnish	Uralic	Finnic	938601
bs	Bosnian	Indo-European	Slavic	921232	et	Estonian	Uralic	Finnic	893074
sl	Slovenian	Indo-European	Slavic	912248	hu	Hungarian	Uralic	Finno-Ugric	920592
mk	Macedonian	Indo-European	Slavic	881176	se	Northern Sami	Uralic	Sami	32289
sk	Slovak	Indo-European	Slavic	878540	vi	Vietnamese	Austroasiatic	Vietic	883581
uk	Ukrainian	Indo-European	Slavic	759826	id	Indonesian	Austronesian	Malayo-Polynesian	881198
sh	Serbo-Croatian	Indo-European	Slavic	209379	ms	Malay	Austronesian	Malayo-Polynesian	819431
be	Belarusian	Indo-European	Slavic	61862	mg	Malagasy	Austronesian	Malayo-Polynesian	292520
fr	French	Indo-European	Romance	963140	km	Khmer	Austroasiatic	Khmeric	101294
es	Spanish	Indo-European	Romance	929677	zh	Chinese	Sino-Tibetan	Sinitic	954358
it	Italian	Indo-European	Romance	928427	my	Burmese	Sino-Tibetan	Lolo-Burmese	5326
pt	Portuguese	Indo-European	Romance	919755	th	Thai	Kra-Dai	Tai	892433
ro	Romanian	Indo-European	Romance	913451	ko	Korean	Koreanic		892064
ca	Catalan	Indo-European	Romance	633826	ja	Japanese	Japonic		886850
gl	Galician	Indo-European	Romance	353596	eu	Basque	Language isolate		786645
wa	Walloon	Indo-European	Romance	48894	eo	Esperanto	Constructed		257560
oc	Occitan	Indo-European	Romance	27773	ka	Georgian	Kartvelian		240335

Table 8: Detailed information of OPUS-100 datasets. #Train indicates the number of training instances.